Dynamic ionization of water under extreme conditions

A. F. Goncharov, N. Goldman, L. E. Fried, J. C. Crowhurst, I-F. W. Kuo, C. J. Mundy, J. M. Zaug

July 27, 2004

Disclaimer

Dynamic ionization of water under extreme conditions

Alexander F. Goncharov, Nir Goldman, Laurence E. Fried, Jonathan C. Crowhurst, I-Feng W. Kuo, Christopher J. Mundy, and Joseph M. Zaug.

Lawrence Livermore National Laboratory, University of California

Raman spectroscopy has been used to study fluid water at approximately 1000 K and 2 to 60 GPa in a laser heated diamond anvil cell. First principles molecular dynamics (MD) simulations have also been employed to simulate water under similar conditions. The experimental Raman intensity of the O-H stretch mode was observed to decrease with pressure, and beyond 50 GPa this mode was no longer visible. At approximately the same pressure we inferred a change in the slope of the melting curve. Consistent with these experimental observations, the MD simulations show that water under these conditions forms a *dynamically ionized liquid* state, which is dominated by very short lived (<10 fs) H_2O, H_3O^+ and O^{2-} species.

PACS number(s): 62.50.+p, 61.20.Ja, 64.70.Ja, 78.30.Cp

The behavior of fluid water at extreme conditions of high pressure and temperature is of fundamental importance to the planetary and geosciences, fundamental chemistry, environmental science, and biology. A key question, in particular, is the pressure and temperature induced dissociation of water, and its corresponding chemical composition and structure. This question has previously been addressed mainly theoretically [1-3]. A superionic phase of water has been observed in simulations above 20 GPa and 2000 K. In this case oxygen atoms form a lattice, which is isostructural to crystalline ice VII, while protons hop between different molecular sites [1]. Contrary to this conclusion, calculations performed more recently [3] show large oxygen diffusion at two-fold compression (corresponding to a pressure of about 22 GPa) characteristic of a fluid state.

Until recently, the experimental study of water at extreme conditions was limited mainly to shock–wave compression investigations [4,5]. Electrical conductivity shows a rapid increase up to 30 GPa but only a weak dependence at higher pressures. This fact has been imputed to chemical ionization. The results of a Raman study of shock-compressed water [5] show the persistence of H_2O molecules and near absence of hydrogen bonding (dominant at 12 GPa) at 26 GPa. Static diamond anvil cell (DAC) experiments have been mostly limited to the solid phase below the melting curve (ice VII above 2 GPa) and also the melting curve itself [6-10]. No characterization of the high-temperature state has been performed. Raman measurements of liquid water under static high-pressure conditions have up to now been limited to 6 GPa [11].

In this letter, we present Raman data of ice and liquid water obtained *in situ* using a laser heated DAC over a wide range of pressure and temperature. The results show that hydrogen bonds weaken substantially in the solid state prior to melting. The Raman spectra of the liquid are qualitatively similar to those measured in shock-wave experiments [5], but there is a difference in the spectral position of the peak associated with the hydrogen-bonded molecules. Our most important observation is that the O-H stretch mode broadens and disappears above 50 GPa, and that there is a concomitant change of the slope of the melting curve. We believe these phenomena to be manifestations of molecular dissociation. First principles simulations are used to aid in the interpretation of the spectra. These simulations indicate a transition to a dynamically ionized phase dominated by "transient" H_2O, H_3O^+, and O^{2-} species at 50 GPa.

We performed the experiments using a DAC with diamonds having flats of between 200 and 500 μm diameter depending on the required pressure. A rhenium gasket was used to contain the sample. A continuous-wave 50 W Nd:YAG laser was used as the heating source. To provide efficient heat transfer to the sample we placed in the gasket cavity a 50x50 μm plate of a Pt-Ir (20% Ir) alloy with a central hole of diameter of approximately 10 μm. This hole formed a sample cavity that ensured radially symmetric heating. In order to further reduce thermal gradients, the sample was thermally insulated from the diamond anvils by smooth alumina plates of approximate thickness 5 μm. In the experiments described below the Raman spectra did not show any sign of chemical reaction. Our confocal Raman system has previously been described in detail [12]. We used the 458 nm line of a 300 mW Ar ion laser to excite the Raman spectra. A Mitutoyo near IR 20x long-working distance lens was employed for the collection of Raman spectra in the backscattering geometry. The Raman spectra were collected in the range of −1000 to 4000 cm^{-1} in one spectral window. The YAG laser radiation was injected into the Raman system using polarizing beam-splitter cubes and was focused to a 20-30 μm spot using the same objective lens. The heating laser power was increased in steps (by rotating a λ/2 wave plate coupled to a polarization cube).

We attempted to determine temperature of the sample by fitting the Planck function to the emitted thermal radiation. We also estimated temperature by analyzing the relative intensities of the Stokes and Anti-Stokes peaks of the intermolecular (phonon) mode with a maximum at between 300-500 cm^{-1}. We found that this method yields substantially lower temperatures compared to the radiometric method. We adopted the second

technique because it is based on an intrinsic property of the studied system and, moreover, because it gives results that are more consistent with other observations (see below). Pressure was determined at room temperature using a conventional ruby manometer before and after laser heating (which was the same within the experimental error in most cases). Thermal pressure due to laser heating was estimated not to exceed 1 GPa and was neglected for simplicity [6,13].

The Raman spectra of the ice VII (proton disordered) solid phase show a drastic change upon heating in the region of the O-H stretch (Fig. 1). In the ice VII phase this band is split into three components $\nu_1(A_{1g})$, $\nu_3(E_g)$ and $\nu_1(B_{1g})$ (enumerated here in the proton-ordered ice VIII notation) [14]. Under pressure the frequencies of this O-H multiplet soften, and this may be ascribed to strengthening of the hydrogen bond [15,16]. The frequencies of all three components of the O-H band increase with temperature indicating that the hydrogen bonds weaken in ice VII as the melting transition is approached. To determine the melting of ice VII, we monitored the behavior of the phonon mode. This band broadens drastically when melting occurs [17], while in the solid phase the corresponding degree of temperature-induced broadening is very moderate. Concomitantly, changes also occur in the O-H band: a broad doublet is observed in the liquid with a different intensity distribution compared to that in ice VII. The position of the high-frequency band corresponds to that of free water molecules, while that of the lower-frequency band may be assigned to hydrogen-bonded molecules [18].

First principles Car-Parinello [19] density functional MD simulations of liquid water were conducted at 1500 K and 2000 K with a fixed volume. We used CPMD v.3.82 [19], with the BLYP exchange correlation functional [20], Troullier-Martins pseudo-potentials [21] for both oxygen and hydrogen, and a system size of 54 H_2O molecules. A plane wave cutoff of 85 Ry was used in all simulations. The temperature was controlled with Nose-Hoover thermostats [22] for all nuclear degrees of freedom. A value of 200 au was chosen for the fictitious electron mass. The simulation time step was 0.048 fs. Simulations were performed at densities of 2.0-2.4 g/cc, with a step of roughly 0.1 g/cc between neighboring densities. Equilibration runs were performed for 2 ps at each density studied, starting from a configuration at a lower density. Data collection runs were performed for 5-10 ps.

Molecular concentrations and lifetimes were analyzed on the basis of the O-H bond distance. The O-H bond distance cutoff was determined to be the position of the maximum in the O-H potential of mean force at the simulated density and temperature. In Figure 2 we show that at 2.0 g/cc (21 GPa), H_2O is the dominant species, with the presence of short-lived H_3O^+, OH^-, and O^{2-}. This is consistent with simulations at nearly the same conditions of Schwegler $et\ al.$ [3]. At 2.2 g/cc (33 GPa), however, the concentration of ionic species increases to become similar to that of neutral H_2O. A mixture of charge carriers is found at this condition. Finally, at 2.4 g/cc (49 GPa), there is a change in the nature of the anionic charge carriers. The concentration of OH^- drops precipitously, while O^{2-} becomes the principle carrier of negative charge. The proton concentration also decreases while H_3O^+ becomes the principle carrier of positive charge.

At 2.4 g/cc all species lifetimes are found to be 10 fs or less. This is less than an O-H

bond period, so the system consists entirely of short-lived "transition states". This

dynamically ionized fluid phase of water has not been previously encountered.

Preliminary calculations above 2.4 g/cc show freezing into a glass-like state with mobile

protons, in agreement with the superionic phase predicted in Ref. [1].

Under pressure Raman spectra of liquid water decrease in intensity in the spectral range

of the O-H stretch vibration and exhibit a change in line shape (Fig. 3). The higher

frequency component depends only weakly on pressure, while the lower frequency peak

softens and broadens (Fig. 4), and finally become unobservable above 30 GPa. The

pressure dependence of this band (Fig. 4) follows closely that of the soft mode in ice

VIII, which is a precursor of the transition to ice X (having symmetric hydrogen bonds)

[16]. This fact supports the interpretation of the Raman O-H stretch doublet in the liquid

phase mentioned above [11]. In contrast, the phonon mode shows a frequency shift with

pressure similar to that observed in ice VII and VIII [14,16] and no other apparent

change.

The Raman spectra of liquid water under extreme conditions are qualitatively similar to

those observed in shock compression experiments [5]. The difference in the spectral

position of the lower-frequency component (Fig. 4) can be explained by the temperature

dependence of this band [11] and the fact that the experiments were performed at

different temperatures. A relative decrease of intensity of the lower-frequency component

in the experiment of Ref. [5] is consistent with our observations (Figs. 3,4). At low

pressure our data match the results of static experiments [11]. Our Raman spectra are also in agreement with theoretically computed power spectra at 1500 K (Fig. 3). The computed power spectra predict an almost total disappearance of the O-H stretch band in dense, hot water at 1500 K, which is in agreement with the experiment.

The observed changes in Raman spectra of liquid water with pressure imply alteration of the local atomic structure and in the bonding properties. Below 30 GPa liquid water partly preserves hydrogen bonding, so some H_2O molecules are bound and form small clusters or chains. At higher pressure one can see a broadening and eventual disappearance of the O-H stretch. This is consistent with a theoretically predicted increase of mobility (i.e. diffusivity) of hydrogen atoms [3], which results in a decrease of the lifetime of the H_2O molecule (Fig. 2). In this regime the proton is able to easily hop from one molecule to another. Above 50 GPa, no O-H stretch could be observed, which indicates a dissociation of H_2O molecules. This regime is qualitatively similar to a dynamically proton disordered "ionized" ice VII [23] or the "transition region" referred to in Ref. [16]. At even higher pressure a centering of the hydrogen bond implies a transition to a nonmolecular solid [16]. One can expect that the corresponding molten state should be qualitatively similar and may possess some features of the superionic phase [1].

Using Raman diagnostics, we have investigated the phase diagram of water at high temperature (Fig. 5). We determined melting by observing characteristic Raman spectra corresponding to each state of matter (c.f., Refs. [6,8,10]). Our data agree within the

accuracy of our measurements with the results of Refs. [6-8,10]. The melting curve shown in Fig. 5 suggests a change in slope above 50 GPa and 800 K. Similar behavior was observed in Ref. [9] and interpreted as being due to the presence of the triple point between liquid water, ice VII and ice X (albeit at substantially higher temperature). Based on experimental and theoretical results [17,23,24] we would instead propose the dynamically disordered ice VII as the high-pressure solid phase. Our results show that water exhibits a continuous transition in the same pressure range. The high-pressure liquid phase corresponds to the newly defined *dynamically ionized liquid water*. This suggestion is based on the experimental trends (Fig. 3) and also theoretical modeling.

In conclusion, our combined experimental and theoretical investigation of water above the melting line shows that it gradually transforms from a molecular to a dynamically ionized state above 50 GPa. First principles MD simulations indicate that this a fluid phase consisting of H_2O, H_3O^+, and O^{2-} "transition states" with lifetimes less than 10 fs. This work demonstrates the value of the in situ high-temperature Raman method to study phase diagrams and material properties under extreme conditions.

Bibliography.

[1] C. Cavazzoni, G. L. Chiarotti, S. Scandolo, *et al*., Science **283**, 44 (1999).

[2] E. Schwegler, G. Galli, and F. Gygi, Phys. Rev. Lett. **84**, 2429 (2000).

[3] E. Schwegler, G. Galli, F. Gygi, and R. Q. Hood, Phys. Rev. Lett. **87,** 265501 (2001).

[4] A. C. Mitchell and W. J. Nellis, J. Chem. Phys. **76**, 6273 (1982); R. Chau, A. C. Mitchell, R. W. Minich, and W. J. Nellis, J. Chem. Phys. **114**, 1361 (2001).

[5] N. C. Holmes, W. J. Nellis, and W. B. Graham, G. E. Walrafen, Phys. Rev. Lett. **55**, 2433 (1985).

[6] Y. Fei, H.-K Mao, and R. J. Hemley, J. Chem. Phys. **99**, 5369 (1993).

[7] F. Datchi, P. Loubeyre, R. LeToullec, Phys. Rev. B **61**, 6535 (2000).

[8] N. Dubrovinskaia and L. Dubrovinsky, High Pressure Res. **23,** 307 (2003).

[9] B. Schwager, L. Chudinovskikh, A. Gavriliuk and R. Boehler, J. Phys.: Condens. Matter **16**, S1177 (2004).

[10] M. Frank, B. Militzer, Y. Fei *et al*., unpublished.

[11] T. Kawamoto, S. Ochiai, H. Kagi, J. Chem. Phys. **120**, 5867 (2004).

[12] A. F. Goncharov, V. V. Struzhkin, R. J. Hemley, H-K. Mao, Z. Liu. In Science and Technology of High Pressure, edited by M. H. Manghnani, W. J. Nellis, and M. F. Nicol (Universities Press, Hyderabad, India, 2000), pp. 95-99.

[13] A. Dewaele, G. Fiquet, and Ph. Gillet, Rev. Sci. Instrum. **69**, 2421 (1998).

[14] K. P. Hirsch and W. B. Holzapfel, J. Chem. Phys. **84,** 2771 (1986).

[15] G. E. Walrafen, M. Abebe, F. A. Mauer et al., J. Chem. Phys. 15, 2166 (1982).

[16] A. F. Goncharov, V. V. Struzhkin, H-K Mao, and R. J. Hemley. Phys. Rev. Lett. **83,** 1998 (1999).

[17] The phonon mode broadens substantially above 52 GPa, and so this criterion could no longer be used. At 52-79 GPa and elevated temperatures our Raman spectra show a decrease in intensity of the overdamped O-H stretch mode at approximately 1500 cm^{-1} [16,19] and no obvious frequency shift. This is consistent with the covalent character of the bonds of the high-pressure phase (see text).

[18] Raman spectra of liquid water have been debated extensively in the literature. Although the interpretation is still controversial, we adopted here most recent point of view [11], which is consistent with the present observations (see text).

[19] R. Car and M. Parrinello, Phys. Rev. Lett. **55**, 2471(1985); CPMD, version 3.7: copyright IBM Corp., 1900-2003, copyright Tro MPI fuer Festkoerperforschung Stuttgart, 1997-2001;www.cpmd.org.

[20] A. D. Becke, Phys. Rev. A, **38**, 3098(1988); C. Lee; W. Yang, R. C. Parr, Phys. Rev. B **37**, 785 (1988).

[21] N. Troullier and J. Martines, Phys. Rev. B **43**, 1993 (1991).

[22] S. Nosé, Mol. Phys. **52**, 255(1984); W. G. Hoover, Phys. Rev. A **31**, 1695 (1985).

[23] M. Benoit, A. H. Romero, and D. Marx, Phys. Rev. Lett., **89,** 145501 (2002).

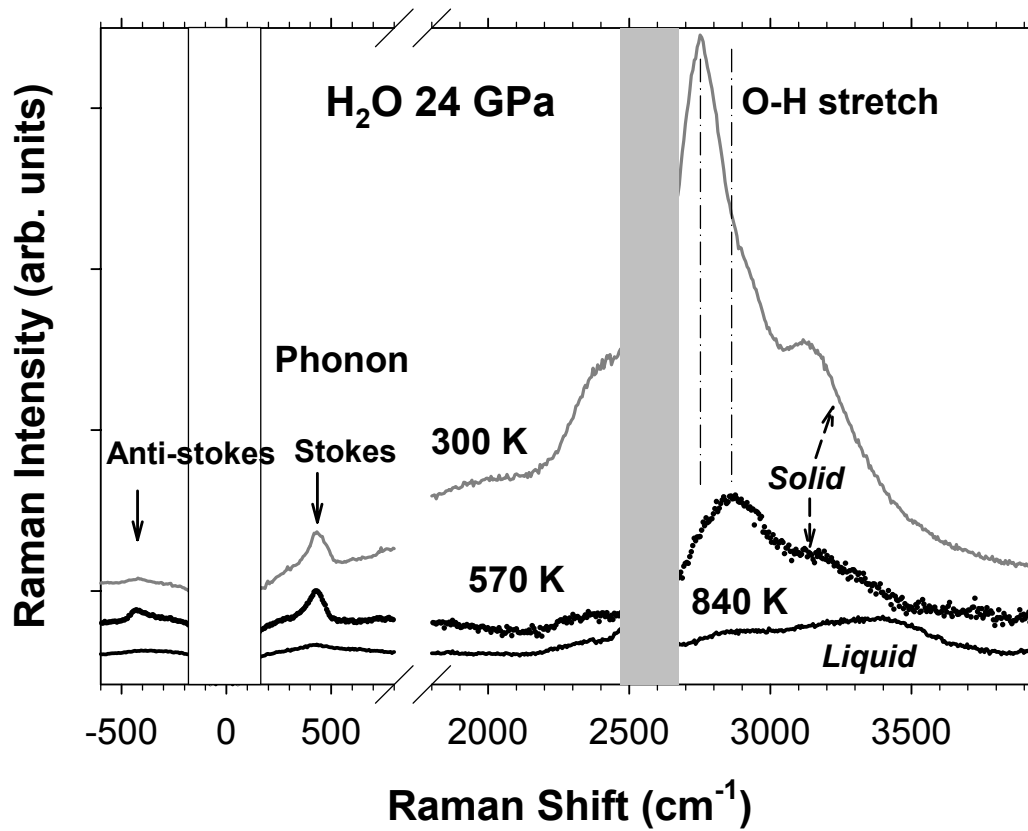[24] A. Putrino, M. Parrinello, Phys. Rev. Lett., **88,** 176401 (2002).

Figures

Fig. 1. The temperature dependence of Raman spectra of H_2O. The pressure measured at room temperature is 24 GPa. The Raman signal corresponding to the second order scattering from the diamond anvils is subtracted [16]. The shaded area masks an uncertainty in this procedure in the vicinity of the diamond second-order peak. The rectangle centered at zero frequency masks differential peculiarities associated with the subtraction of elastically scattered radiation.
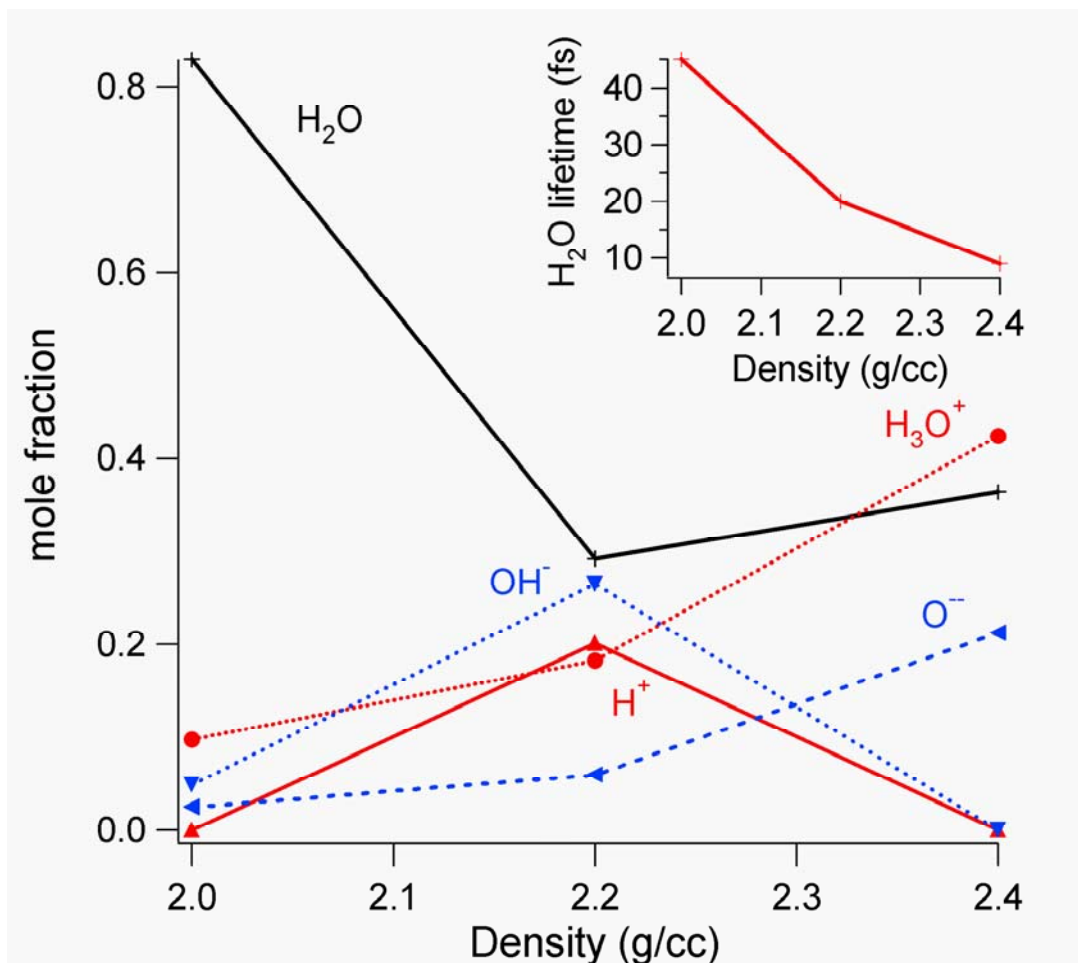
Fig. 2: Calculated concentrations of species present during water simulations at 2000 K. Inset: the lifetime of an H_2O molecule as a function of density at 2000 K. All other species lifetimes were found to be less than 10 fs.
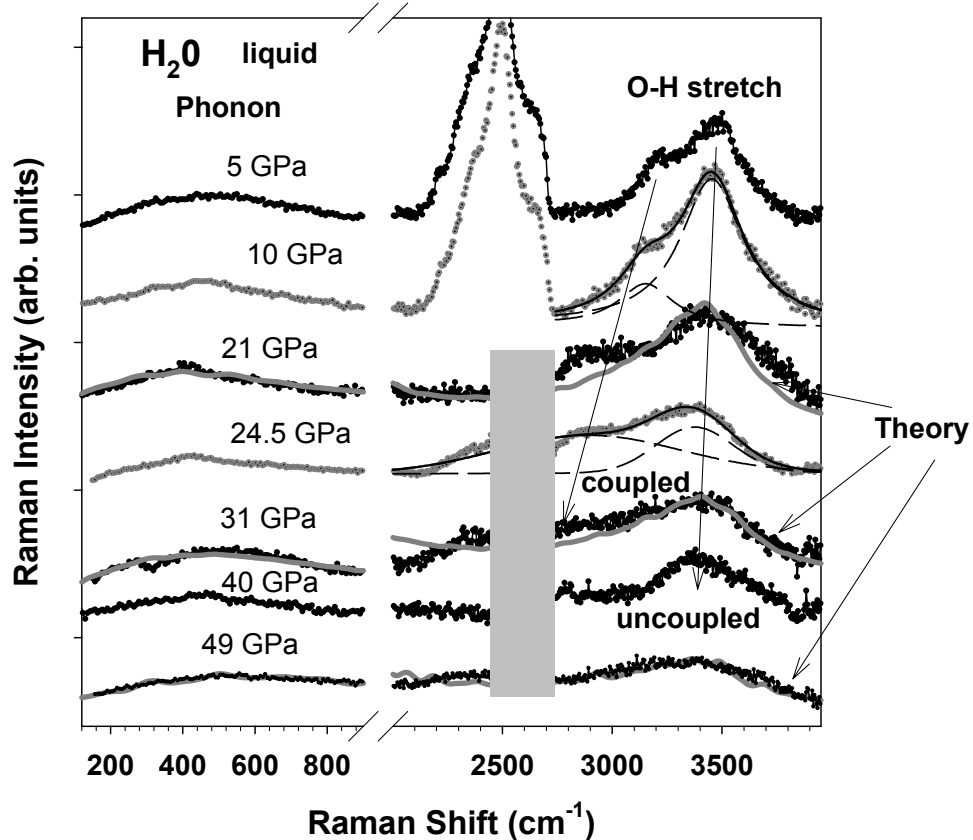
Fig. 3. Raman spectra of liquid water as a function of pressure. The Raman signal corresponding to the second order scattering from the diamond anvils is subtracted for traces corresponding to pressures above 10 GPa. Thin solid lines are phenomenological fits, long-dashed lines correspond to the individual components. Explanation of the shaded area is the same as in Fig. 1. Thick gray lines represent theoretically computed power spectra at 1500 K, scaled in intensity to better match observations.
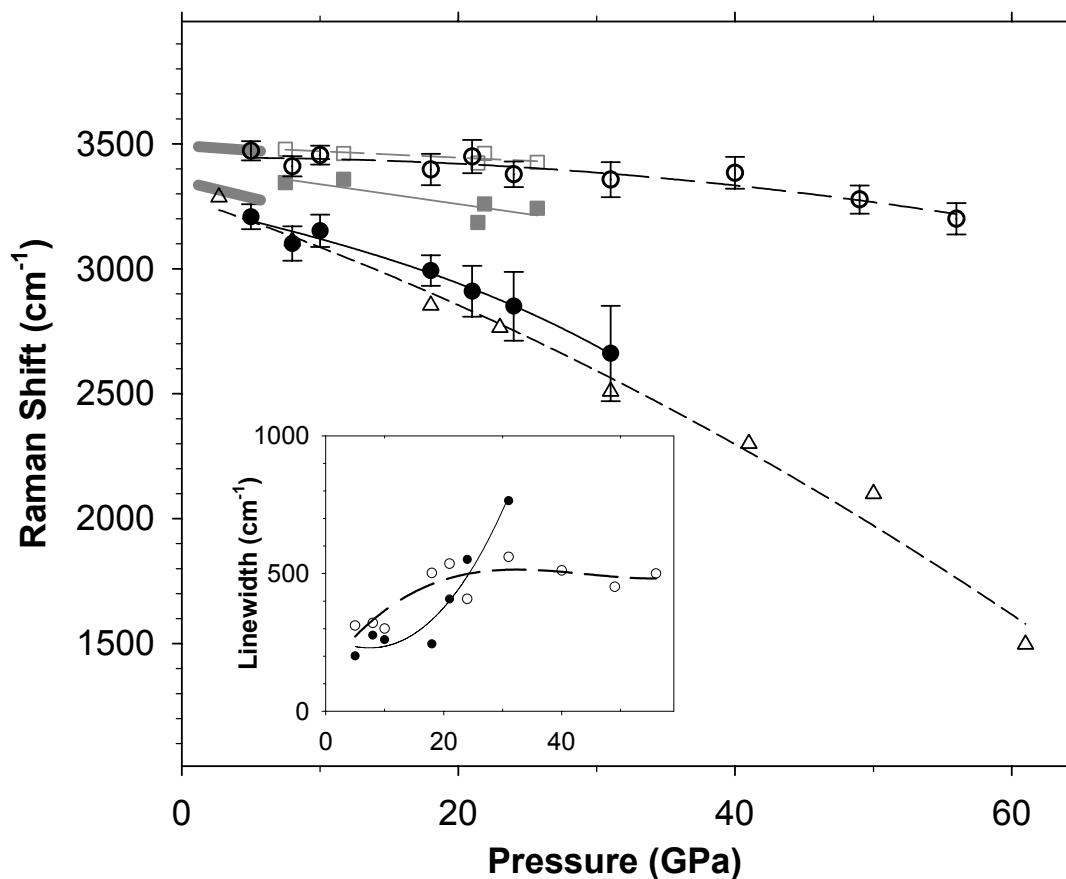
Fig. 4. Raman O-H stretch frequencies of liquid water as a function of pressure. Open and solid circles are the data from this work; open triangles are low- temperature data (ice VIII) from Ref. [16]. Gray squares are shock-wave data from Ref. [5]. Lines are guides to the eye. Thick solid gray lines are interpolations of the static compression data of Ref. [11]. The inset shows the pressure dependences of the line width for the O-H stretch components.
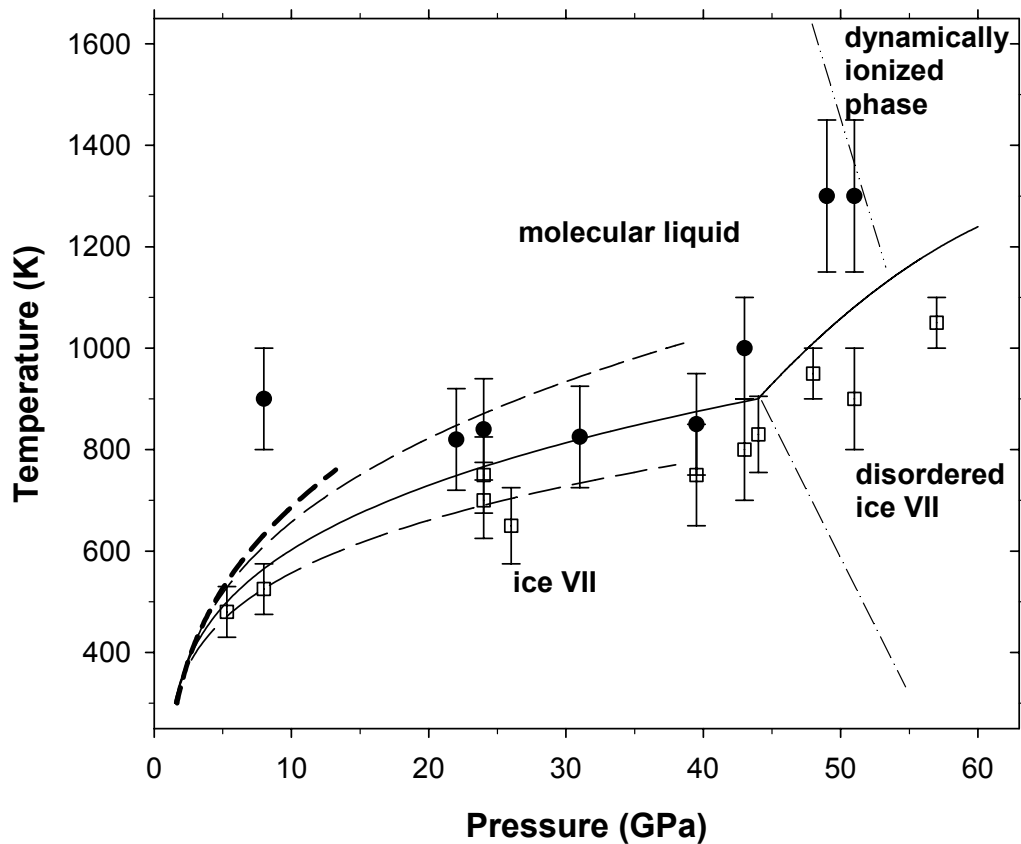
Fig. 5. Melting curve of H_2O. Open squares and solid circles correspond to the solid and liquid phases, respectively. Solid lines are guides to the eye for our results. Dashed-dotted lines are our suggested phase boundaries (see text). Gray dotted, long dashed and medium dashed lines are interpolated data from Refs. [7,10,8], respectively. Data from the Ref. [9] are much higher in temperature and are not shown.